Asociación Argentina
de Mecánica Computacional

Mecánica Computacional Vol XXVII, págs. 249-264 (artículo completo)
Alberto Cardona, Mario Storti, Carlos Zuppa. (Eds.)
San Luis, Argentina, 10-13 Noviembre 2008

LARGE-EDDY SIMULATION OF THE FLOW AND THERMAL FIELDS PAST A CIRCULAR CYLINDER

Hugo D. Pasinato

Dpto. Ing. Química,
RAC, Universidad Tecnológica Nacional,
Plaza Huincul, Neuquén, hpasinato@uacf.utn.edu.ar,
http://www.uacf.utn.edu.ar

Keywords: Heat transfer; Separated Turbulent Flow; Large-Eddy Simulation; Numerical Simulation.

Abstract. Flow with heat transfer around a circular cylinder at Reynolds number 3900 and Prandtl number 0.71 was studied using large eddy simulation, LES. The main goal of this work was to look at the prediction of heat transfer in a separated turbulent flow, using techniques used in applied problems in engineering for separated turbulent flow. The computations are carried out with a central second-order finite-volume method, with the Smagorinsky-Lylli turbulence model, and a constant turbulent Prandtl number equal to 0.80 for turbulent heat modeling. The results are compared with previous numerical results and experimental data from the literature. The flow fields is in acceptable agreement with similar numerical results, although the turbulence level farther downstream in the wake is under predicted in comparison with previous results using high-order accurate numerical method presented in the literature. In order to check the heat transfer prediction global mean Nusselt number and local Nusselt number were used. Although mean values for global Nusselt number present error in the order of 20% with experimental data, which can not be considered as catastrophic, the local heat transfer prediction exhibits a poor performance in the separated region, mainly because the numerical solution does not follow the trend of the experimental local Nusselt number distribution around the cylinder.

1 INTRODUCTION

Some of the most challenging applications of computational turbulent heat transfer are those in complex geometries. For instance, the prediction of heat transfer in separated turbulent flow remains a challenge in practical situations, in contrast to velocity field prediction, which has concentrated the attention for several years.

Separated flows are far from equilibrium and the analogy between momentum and heat transfer fails. Thus the use of a constant turbulent Prandtl number based on the Reynolds analogy for heat transfer prediction can be very inaccurate (Spalart and Strelets, 2000; Kong, Choi, and Lee, 2001; Inaoka, Yamamoto, and Suzuki, 1999).

One of these applications to complex geometries is the flow past a circular cylinder. Experimental and numerical results from cylinder in cross flow have been widely reported (Lourenco and Shih, 1993; Rajagopalan and Antonia, 2003; Beaudan and Moin, 1994; Mittal, 1995; Breuer, 1998; Kravchenko and Moin, 2000; Hansen and Long, 2002; Young and Ooi, 2007; Catalano et al., 2003). A case in point is the sub-critical flow past a circular cylinder at a Reynolds Number of 3900, which has became a flow field test case owing to the number of experimental and numerical studies. Using this test case different aspects of separated turbulent flow numerical simulation have bee studied, like as the performance of structured and unstructured grids (Hansen and Long 2002), the importance of numerical dissipation and the suitability of upwind-biased versus second-order centered schemes (Beaudan and Moin, 1994; Mittal, 1995; Breuer, 1998; Kravchenko and Moin, 2000), and also technique and modeling aspects like as the performance of RANS, Reynolds Averaged Navier-Stokes Equations, unsteady RANS, Large Eddy Simulations, LES, and URANS/LES techniques like as DES, Detached Eddy Simulations (Breuer 1998; Catalano et al. 2003; Young and Ooi 2007).

The main and most important conclusions from the previous numerical works have been the importance of numerical dissipation in these kind of simulations, and the relative low importance of turbulence models. At least for this low-Reynolds turbulent flow. For example that high-order upwind biased schemes, which has been efficiently used for DNS transition and turbulence in boundary layers, present high level of numerical dissipation overwhelming in certain region farther downstream of the cylinder the contributions from the subgrid-scale eddy viscosity model. Moreover, that second-order centered schemes, which in contrast do not exhibit numerical dissipation and therefore have not spurious damping of small scales, are extremely sensitive to grid stretching owing to dispersive errors (Mittal, 1995). On the other hand, as regarding turbulence models, although the dynamic version of the Smagorinky model has proved to be relatively more accurate, the Smagorinky model with a wall treatment has presented results with the same level of precision (Breuer, 1998). Thus the conclusions about velocity field prediction of this low-Reynolds flow past a circular cylinder with LES seems to be that is relevant the use of a balanced structured grid with a good near-wall resolution of the boundary layer, a centered second order centered scheme, with the dynamics Smagorinsky turbulence model with a wall treatment.

Based on previous works, therefore, it seems that in order to simulate the subcritical turbulent flow past a circular cylinder at the low-Reynolds number of 3900, a reasonable numerical technique is the use of a centered second order scheme, and the use of the LES technique with the dynamic Smagorinsky model with some treatment at the wall. It is important to mention that LES is a suitable technique only for this low-Reynolds number turbulent flow. It should be noted however, that for engineering applications of high Reynolds flows, RANS/LES techniques should be used owing to the near-wall grid requirement imposed by LES.

Thus in the present work the goal is to present the first numerical results of an investigation of the flow and thermal fields past a circular cylinder in a cross flow at a subcritical low-Reynolds number. Based on previous works a finite volume method in cylindrical coordinates, with a second-order centered numerical scheme has been used. For turbulence, in this first results of heat transfer in separated turbulent flow, the Smagorinsky model with a van Driest treatment for eddy viscosity at the wall was used. The Reynolds of the flow was $3,900$, and the molecular and turbulent Prandtl numbers are 0.71 and 0.80,

respectively.

2 NUMERICAL METHOD

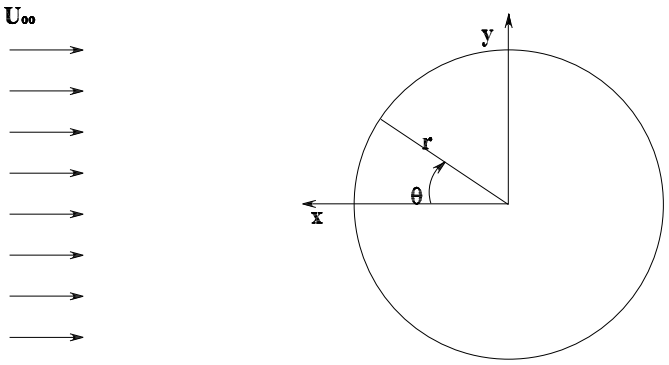

Figure 1: Coordinate systems used, with z into the plane.

The unsteady incompressible Navier-Stokes and energy equations were numerically solved for the flow and thermal field around a circular cylinder for $Re = DU_\infty\rho/\mu = 3,900$, with molecular and turbulent Prandtl numbers equal to $Pr = 0.71$, and $Pr_t = 0.80$, respectively. Where U_∞ is the far field non-perturbed streamwise velocity, and D is the cylinder diameter. The numerical code is based on the finite volume method, and written in a staggered grid in cylindrical coordinates, $r - \Theta - z$ (Pasinato, 2000). Figure 1 shows the cylindrical coordinates, as used in the numerical simulation, and the Cartesian axes, as used in the post-processing. The code employs second-order central differences in the three directions in space. For time advancement, the fractional step approach, in combination with Crank-Nicholson for viscous and convective terms, is used. Continuity constraint is imposed by solving a Poisson equation for pressure. Velocity, and pressure fields are solved using a simplified multi-grid iterative method.

In the following, for simplicity, only reference to Cartesian axes and velocities used in the results presentation are given. Then in this paper, u, v, and w are the dimensionless instantaneous velocities in the streamwise (x), normal to the far field flow (y), and spanwise (z) directions, respectively. All instantaneous variables are decomposed in a large and small-scale motion, $\bar{u}$, and u', respectively. On the other hand, in order to separate the large and small-scale motion, the three-dimensional, time-dependent Navier-Stokes and energy equations are filtered. In the present study a box filter is applied as a filter kernel.

Then Navier-Stokes and energy equations for an incompressible unsteady flow, written for simplicity, and space reason, in Cartesian coordinates, and taking the temperature field as a passive scalar, are,

$$\frac{\partial \bar{u}_i}{\partial x_i} = 0 \tag{1}$$

$$\frac{\partial \bar{u}_i}{\partial t} + \frac{\partial(\bar{u}_i\bar{u}_j)}{\partial x_j} = \frac{1}{Re}\frac{\partial}{\partial x_j}\frac{\partial(\bar{u}_i)}{\partial x_j} - \frac{\partial \bar{p}}{\partial x_i} - \frac{\partial}{\partial x_j}(\langle u_i u_j\rangle - \bar{u}_i\bar{u}_j) \tag{2}$$

$$\frac{\partial \bar{\theta}}{\partial t} + \frac{\partial(\bar{\theta}\bar{u}_j)}{\partial x_j} = \frac{1}{RePr}\frac{\partial}{\partial x_j}\frac{\partial(\bar{\theta})}{\partial x_j} - \frac{\partial}{\partial x_j}(\langle \theta u_j\rangle - \bar{\theta}\bar{u}_j) \tag{3}$$

where the non-dimensionalization was done using the free-stream velocity U_∞ and the cylinder diameter, D, and the temperature difference $T_W - T_\infty$, as $\theta = (T - T_\infty)/(T_W - T_\infty)$. Where θ is the dimensionless instantaneous temperature, T_W is the wall cylinder temperature, T_∞ is the temperature of the far thermal

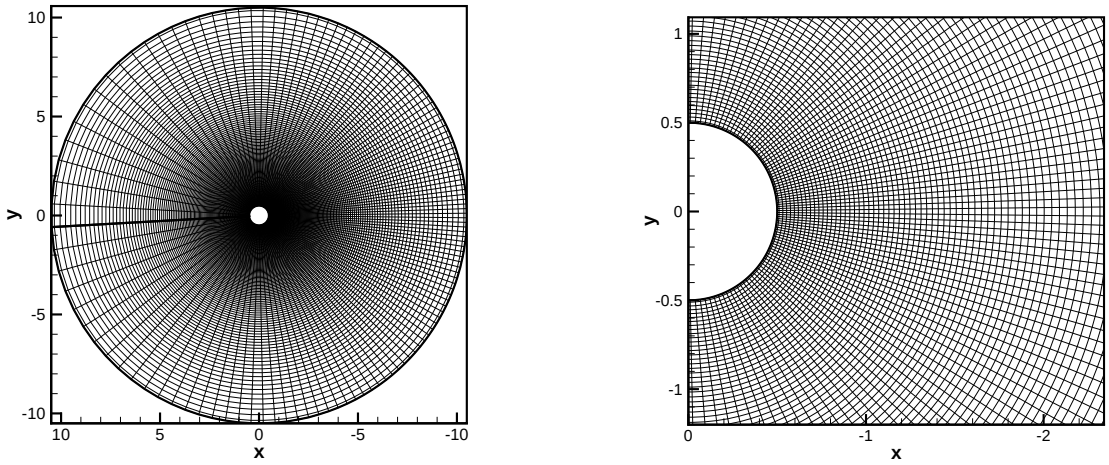

(a) (b)

Figure 2: Numerical grid in a x-y plane with $128 \times 128 \times 16$ cells, which was made with the same stretching coefficients of the grids used in this work. (a) Full grid plane. (b) Cylinder rear near-wall stretching.

field. In these equations Pr and Pr_t are the molecular and turbulent Prandtl numbers, and Re the Reynolds based on the free-stream velocity U_∞ and cylinder diameter, D.

As regarding the subgrid scale, SGS, stress tensor in equation (2), it is modeled by the Smagorinky-Lylli model (Piomelli, 1994), which is based on the Boussinesq's approach, which uses an analogy between the SGS stress tensor and the viscous stress tensor. Then the SGS stress tensor is modeled as a function of the large-scale strain tensor $\bar{S}_{ij}$, as,

$$\tau_{ij}^t - \delta_{ij}\tau_{kk}/3 = \ -2\nu_t \bar{S}_{ij} \tag{4}$$

where,

$$\tau_{ij}^t = (\langle u_i u_j \rangle - \bar{u}_i \bar{u}_j) \tag{5}$$

and the eddy viscosity ν_t is modeled based on the Boussineq's approach as a function of the strain rate tensor $|\bar{S}_{ij}|$ in the following way,

$$\nu_t \ = \ l^2 \ |\bar{S}_{ij}| \tag{6}$$

where

$$|\bar{S}_{ij}| \ = \ \sqrt{2 S_{ij} S_{ji}} \tag{7}$$

and the subgrid length l is evaluated proportional to the filter width as,

$$l \ = \ C_S \ \bar{\Delta} \ = \ C_S \ (\Delta x \ \Delta y \ \Delta z)^{1/3} \tag{8}$$

where C_S is the called Smagorinsky's constant.

The first value proposed for this constant has been 0.23 (Piomelli, 1994). However this value was found to damp the turbulent fluctuations excessively, thus a lower value $C_S = 0.1$ has been finally employed for high Reynolds turbulent flows. And this was the value used in the present work.

In order to account for the reduction of the subgrid length scale l in the near-wall region, l is multiplied by a van Driest damping function as,

$$l \;=\; C_S\,\bar{\Delta}\,[1 - exp(-y^+/25)]^{0.5} \tag{9}$$

where $y^+ = yu_\tau/\nu$, with y as the wall distance, and u_τ the friction velocity evaluated on the cylinder wall, at the same angle and spanwise coordenates.

Then the turbulent heat diffusion term at the right hand side of equation (3) is evaluated using a constant turbulent Prandtl number as $\alpha_t = \nu_t/Pr_t$. Thus the SGS thermal stresses are modeled as a function of the large-scale temperature gradient as,

$$(\langle\theta u_j\rangle - \bar{\theta}\bar{u}_j) = \; -2\alpha_t \frac{\partial\bar{\theta}}{\partial x_j} \tag{10}$$

As regarding boundary conditions, periodic boundary conditions are imposed in the z spanwise direction, and convective boundary condition at the outflow boundary, with the following expression,

$$\frac{\partial\phi}{\partial t} + u_b\frac{\partial}{\partial x}\phi \;=\; 0 \tag{11}$$

where ϕ represents an instantaneous variable of the flow, and u_b is a spanwise mean of streamwise velocity at the boundary.

Table 1: Comparison of mean drag coefficient, C_d, length of wake bubble L_{WB}/D, and global Nusselt, with established results.

Study	Re	Grid	C_d	L_{WB}/D	$\bar{Nu}$
Fornberg(1980)	20	152×156	2.00	0.91	
Fornberg(1980)	40	152×156	1.50	2.24	
Dennis and Chang(1970)	20	152×156	2.05	0.94	
Dennis and Chang(1970)	40	152×156	1.52	2.35	
Present	20	$64 \times 64 \times 1$	2.05	0.97	2.47
Present	40	$64 \times 64 \times 1$	1.54	2.45	3.29
Schlichting(1968)	20	Experimental	2.07		
Schlichting(1968)	40	Experimental	1.50		
Knudsen and Katz(1958)	20	Experimental			2.57
Knudsen and Katz(1958)	40	Experimental			3.36

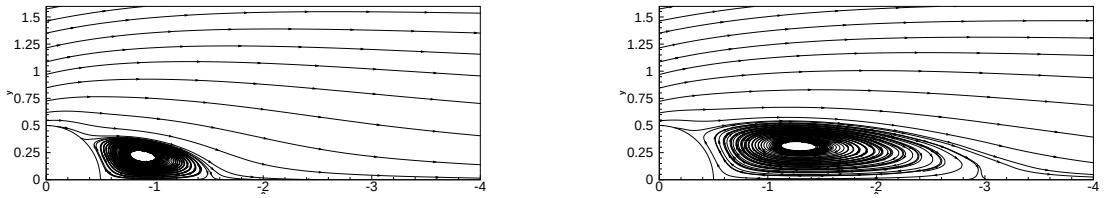

(a) (b)

Figure 3: Stream lines plot for a flow past a circular cylinder at two Reynolds numbers. a) $Re = 20$; b) $Re = 40$.

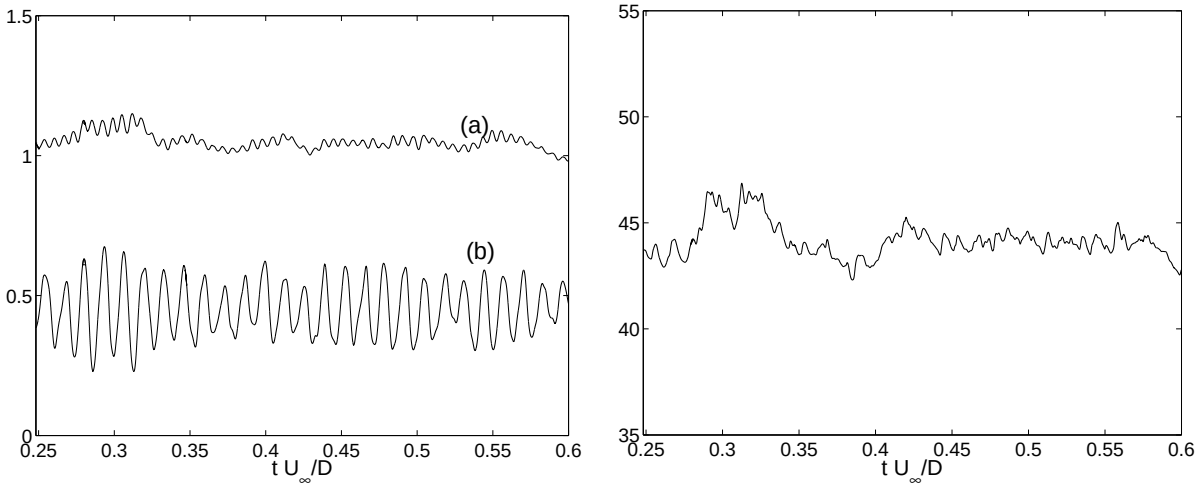

(a) (b)

Figure 4: Typical time distribution of the (a-a) instantaneous drag coefficient $C_d = 2\ Drag\ Force/(DL_z\ \rho U_\infty^2)$; (a-b) friction coefficient $C_f = 2\ \tau_w/(\rho U_\infty^2) \times 30000$, and (b) mean global Nusselt number, $\bar{N}u = \partial((T-T_\infty)/(T_W-T_\infty))/\partial(r/D)_{r=D/2}$.

The computational domain was $21D$ in the $x-y$ plane and πD in the z spanwise directions, the same box used by Breuer (1998), Mittal (1995), and Kravchenko and Moin (2000). For the results presented in this work, this computational domain was discretized with the following 3 grids in $r;\Theta;z$, $144\times144\times24$, $144\times144\times32$, and $152\times152\times40$. Most results presented in this work were obtained with $144\times144\times24$, and $144\times144\times32$ grids. Figure 2(a) and 2(b) show an overall view of the full grid, and of the near-wall region in the cylinder rear for a coarser grid $128\times128\times16$ used in order to interpolate solution in denser grids. All grids, on the other hand, were made with the same stretching coefficients in $r;\Theta$ directions, up to 3% of size difference between two adjacent cells, as suggested by Mittal (1995) for centered schemes. In order to have a good resolution of the boundary layer around the cylinder, the center of the first control volume near the wall were at 5.1, and 4.0 in wall units using the maximum friction velocity around the cylinder for both radial discretizations, respectively. Only small time step, however, of about $0.005D/U_\infty$ was possible to use.

As initial condition, a velocity field from a potential flow was supplied to a $96\times96\times8$ coarser grid, and then this flow was calculated until the mean steady state regime was obtained. Then this flow was interpolated to a denser grid.

After the velocity field is calculated at each time step, the temperature field was obtained integrating the energy equation. For temperature a uniform wall temperature at the cylinder wall was used. The time integration in order to define mean values was taken equal to approximately 140 shedding time periods.

3 RESULTS AND DISCUSSION

3.1 Code validation

Different unsteady and steady cases were solved in order to validate the numerical simulation in cylindrical coordinates for a flow with heat transfer around a cylinder in cross flow. Here two steady cases solved with a very coarse grid are presented. In Table 1 the numerical solution is compared with established results from the literature, and in Figures 3(a)-3(b) the stream lines of the two cases are shown. Although the coarse grid used in these cases it is clear from the mean drag coefficient, C_d, the global Nusselt number $\bar{N}u$, and the stream lines, the good agreement with previous experimental and numerical

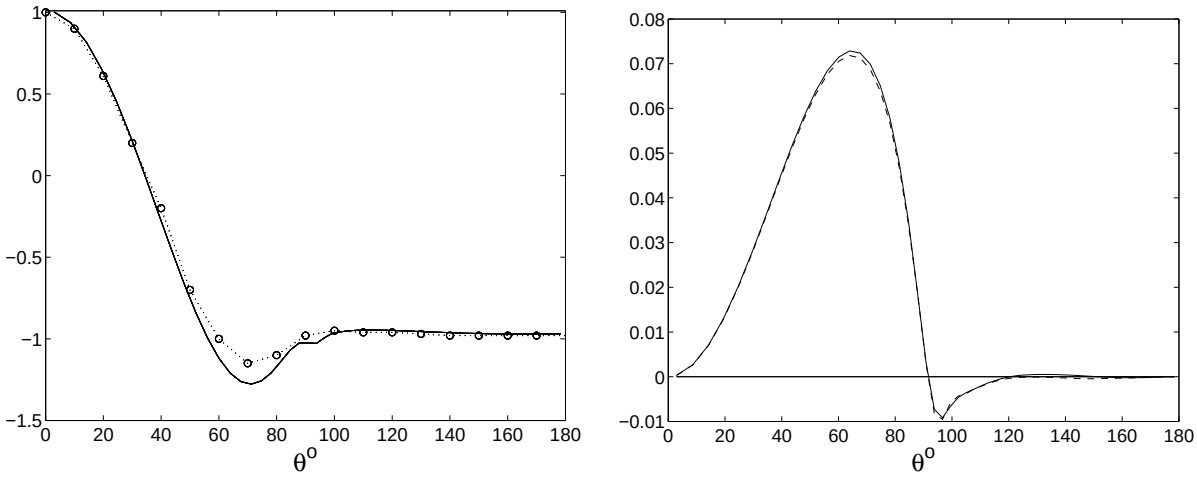

(a) (b)

Figure 5: (a) Distribution of mean pressure coefficient, $C_p = 2\ (P - P_\infty)/(\rho\ U_\infty^2)$. Solid line, Present (RUN3); $\circ \cdot \cdot \circ \cdot \cdot \circ$, exp., Norberg (2000). (b) Friction coefficient, $C_f = 2\ Friction\ force/(DL_z\ \rho\ U_\infty^2)$. Solid line, Present (RUN 3); $- - -$, Present (RUN 2).

data.

3.2 Mean Flow Field

The mean values are defined in space in the spanwise direction and in time, where U and V are the dimensionless mean velocities parallel, (x), and normal, (y), to the far field velocity, respectively.

Figures 4(a)-4(b) show the typical behavior of the instantaneous mean global drag coefficient, C_d, friction coefficient, C_f, and global Nusselt number, $\bar{N}u$. And Figures 5(a)-5(b) show the distribution of the pressure coefficient C_p and friction coefficient C_f around the cylinder. The pressure coefficient has been compared with the experimental values obtained by Norberg (2000), and the agreement is good. And Figures 6(a) the mean streamwise velocity in the centerline of the wake is compared with experimental values, and in Figure 6(b) is shown the vorticy magnitude in a $x - y$ plane for the middle of the spanwise size, at $z/D = \pi/2$. Figures 7(a)-7(b)-7(c), and 7(d), mean streamwise and normal velocity, and Reynolds stress are shown at different planes normal to the streamwise velocity, in the cylinder wake.

In Table 2 the main parameters are compared with other numerical results. These parameters are the drag coefficient,Cd, the dimensionless wake bubble length, L_{WB}/D, the separation angle, Θ_S, the minimum streamwise velocity at the centerline in the cylinder wake, U_{min}, and pressure coefficient at the cylinder rear, Cp_{back}.

For the gross behavior of the flow in general there is a good agreement with experimental data, and with previous numerical results. It should be realized, however, that the study case is a low-Reynolds turbulent flow, for which much of the velocity fluctuations near the cylinder are directly calculated. The root mean square, rms, of the velocities in the cylinder wake afar from the cylinder, whose results are not shown here, have presented an important under prediction of about 30%. It is thought that the dynamic version of the Smagorinsky turbulence model should be used in order to improve it. And, although the grids used in this work are thought to be enough for the gross flow prediction in the neighborhood of the wall, it is thought also that a denser grid should be used in the wake in order to improve rms prediction with a second-order scheme.

For completeness reasons, in the APPENDIX instantaneous fields of the solution are presented.

Table 2: Overview of simulations and parameters of the present work for the turbulent flow past a circular cylinder at $Re = 3,900$, and $Pr = 0.71$, and comparison with other numerical results.

Study	Grid	SGS model	Cd	Cp_{back}	L_{WB}/D	Θ_S	U_{min}.
Breuer(1998)	$165 \times 165 \times 32$	Smag.	1.099	-1.049	1.115	87.9	-0.29
Breuer(1998)	$165 \times 165 \times 32$	Dyn.	1.071	-1.011	1.197	87.7	-0.29
Kravchenko and Moin(2000)	$258 \times 291 \times 48$	Dyn.	1.040	-0.94	1.350	88.	-0.37
Mittal(1995)	$399 \times 100 \times 48$	Dyn.	1.099	-1.049	1.197	88.	
Son and Hanratty(1969)	Experimental		1.099	-1.049	1.197	87.7	
Present (Run 1)	$144 \times 144 \times 24$	- - -	1.210	-1.12	1.350	85.0	-0.37
Present (Run 2)	$144 \times 144 \times 24$	Smag.	1.080	-1.07	1.300	90.8	-0.32
Present (Run 3)	$144 \times 144 \times 32$	Smag.	1.071	-0.98	1.310	89.5	-0.31
Present (Run 4)	$152 \times 152 \times 40$	Smag.	1.068	-0.98	1.310	89.3	-0.31

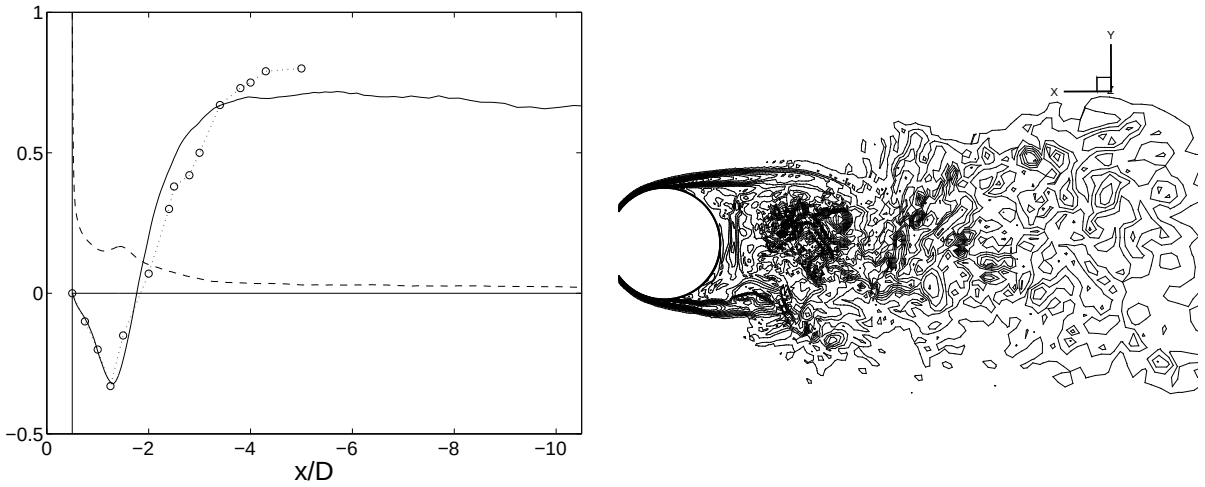

(a) (b)

Figure 6: (a)Mean streamwise velocity $-U/U_\infty$, and temperature $\Theta = (T - T_\infty)/(T_w - T_\infty)$, for the turbulent flow past a circular cylinder at $Re = 3,900$. Solid line, mean velocity, present work; $- - -$, mean temperature, present work; $\circ \cdot \cdot \circ \cdot \cdot \circ$, mean velocity from Lourenco and Shih (1993). A minus sign for mean velocity is used because velocity is going in the x opposite direction. (b)Instantaneous vorticity magnitude at a plane at the middle of spanwise direction, $\omega D/U_\infty$. There are shown 30 contours, from 0.1 to 30.

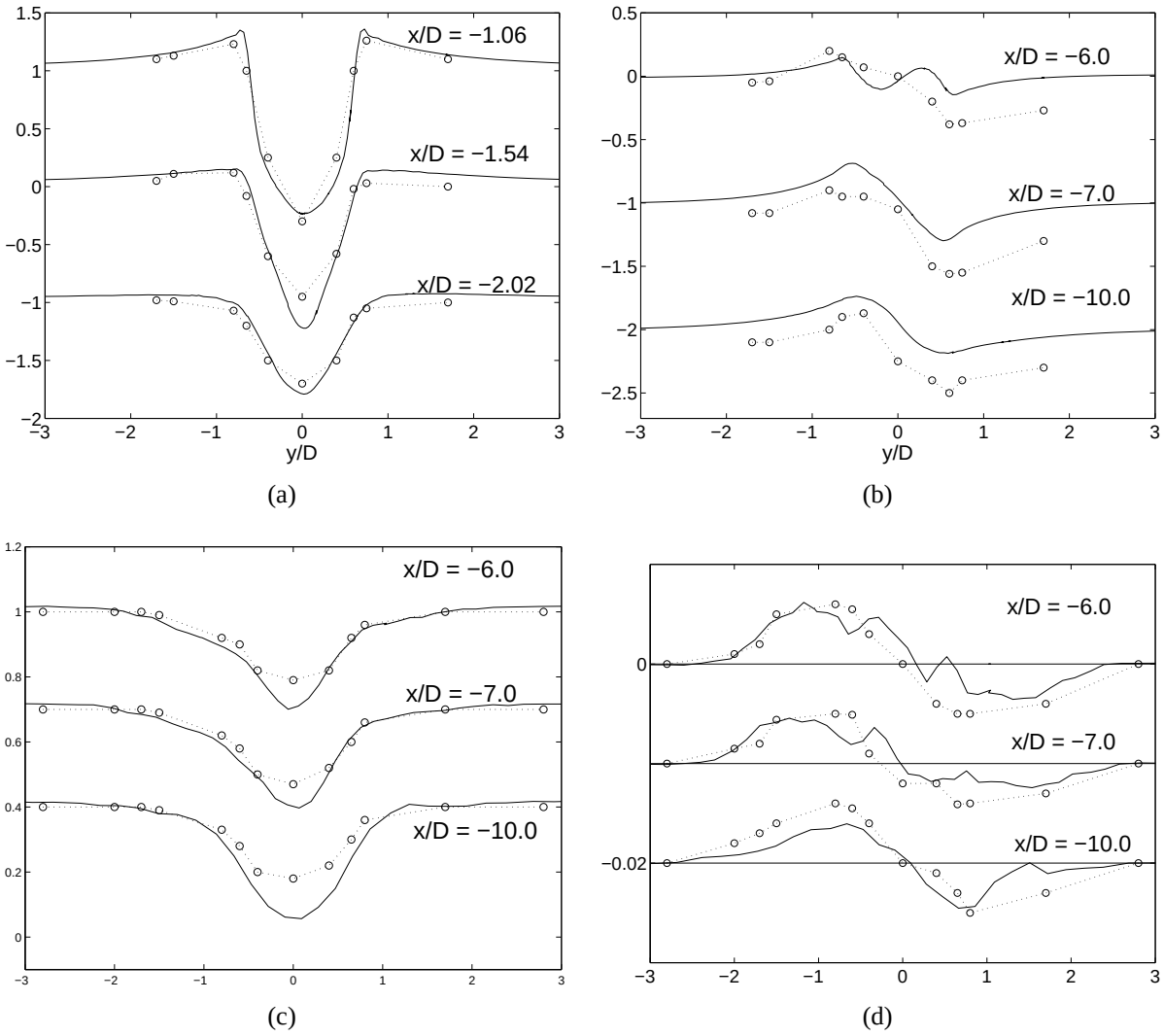

Figure 7: Comparison of dimensionless mean streamwise velocity $-U/U_\infty$, mean normal velocity V/U_∞, and Reynolds stress $\langle u'v' \rangle / U_\infty^2$, for different positions in the wake, for the turbulent flow past a circular cylinder at $Re = 3,900$. Solid line, present work; $\circ \cdots \circ \cdots \circ$, Norberg (2000). (a) Streamwise velocity; (b) Normal velocity; (c) Streamwise velocity, and (d) Reynolds stress.

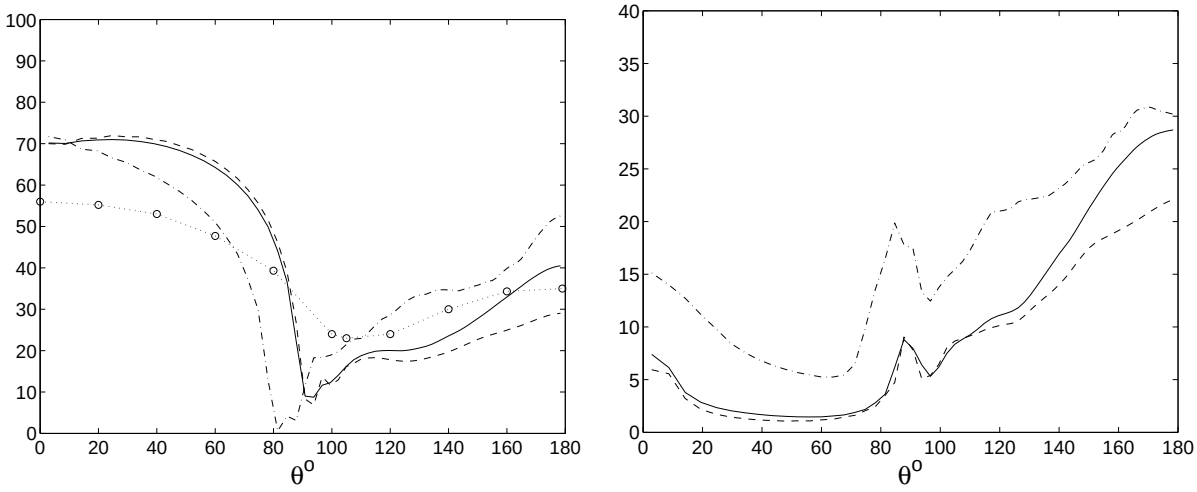

(a) (b)

Figure 8: (a)Distribution of mean local Nusselt number around the cylinder, Nul. Solid line, Present(RUN 3); $---$, Present (RUN 2); $-.-.-$, Present(RUN 1);$\circ\cdots\circ\cdots\circ$, exp., Sarma and Sukhatme (1977), $Re = 3,480$. (b)Distribution of rms of local Nusselt number Nul_{rms} around the cylinder. Solid line, Present (RUN 3); $---$, Present(RUN 2); $-.-.-$, Present(RUN 1).

Table 3: Comparison with experimental data of average Nusselt number, $\bar{Nu}$, Nusselt number at the stagnation point N_0, and Nusselt number at the rear stagnation point N_r, for the turbulent flow past a circular cylinder at $Re = 3,900$, and $Pr = 0.71$.

Study	$\bar{Nu}$	N_0	N_r
Perkin and Lepper(1962)	38.54		
Fand (1965)	35.85		
Sarma and Sukhatme(1977)	40.35	56.82	35
Krall (1969)		58.00	29
Zukauskas and Zigdzda(1985)	32.70		
Sanitjai and Goldstein (2004)	31.08	61.48	
Nakamura and Igarashi (2004)	35.37		18.63
Present (RUN 1)	38.53	72.00	53.00
Present (RUN 2)	43.00	70.00	30.00
Present (RUN 3)	42.30	70.00	41.00

Table 4: Comparison with experimental data of average Nusselt number for the laminar region, $\Theta = 0 - 85^o$, laminar - turbulent transition region $\Theta = 85 - 135^o$, and rear region, $\Theta = 135 - 180^o$, for a turbulent flow past a circular cylinder at $Re = 3900$, and $Pr = 0.71$.

Study	$\bar{Nu}_{(0-85^o)}$	$\bar{Nu}_{(85-135^o)}$	$\bar{Nu}_{(135-180^o)}$
Sanitjai and Goldstein (2004)	52.07	12.32	10.33
Present (RUN 1)	49.62	24.54	41.43
Present (RUN 2)	64.33	16.48	24.70
Present (RUN 3)	63.16	17.68	32.45

3.3 Thermal field

Figures 8(a), and 8(b), show the local Nusselt, and the rms of the local Nusselt around the cylinder. And Table 3, and 4 present the mean global Nusselt, and the mean Nusselt at three regions around the cylinder. The most important from Figure 8(a) is that the distribution of the numerically predicted local Nusselt number around the cylinder, does not follow the trend of the experimental data. From the front stagnation point to the separation point, approximately at $\Theta \approx 90^o$, the mean percentual error is close to 30% for RUN 2 and 3. Then in the vortex region, $85^o < \Theta < 135^o$, the heat transfer is underpredicted in RUN 2 and 3, and overpredicted in RUN 1. And finally in the cylinder rear the calculated values have a reasonable close agreement with experimental data. Part of the error in RUN 2 and 3 in the laminar region of the boundary layer is due to the turbulence model. One of the drawback of Smagorinsky model is that it does not account for laminar to turbulent transition. And in this work the turbulence model was not switch off at any region, the simulations were done with turbulence model in the whole domain. The critical regions are the front stagnation point, and the very near wall region of the boundary layer, where the moduli of the mean strain rate tensor is important, and thus the eddy viscosity of the Smagorisnky model is greater than the molecular viscosity. It is important to note also that from the front stagnation point to downstream, there is a region with an strong favorable pressure gradient, followed by one with an adverse pressure gradient in the vortex region (Figure 5(a)). And it is expected that the turblent diffusion is not well modeled with the constant Prt number in the second region. As it is commented above, in Table 4 the mean Nusselts at three regions around the cylinder are also compared with experimental data. And again in this Table it is clear that there is an overprediction due possibly to the turbulent model, and the use of a constant turbulent Prandtl number.

The first conclusion from previous comparisons is that all calculated global mean values for heat transfer are over predicted in comparison with experimental values. Although global experimental heat transfer coefficients in the literature present some differences, the numerical prediction of global Nusselt number in the present work is greater than every experimental value as it can be noted in Table 3. And most important Figure 8(a) shows that numerical values do not follow the distribution of the experimental data for local Nusselt number.

For completeness reasons, in the APPENDIX some instantaneous flow and thermal fields are presented.

4 CONCLUSION

The flow with heat transfer around a circular cylinder in cross flow at Reynolds number 3900 and Prandtl equal to 0.71 was studied using Large-Eddy Simulation. The main goal of this work was to look at the prediction of heat transfer in a separated turbulent flow, using some simple technique as the used in applied problems in engineering.

The main conclusion are that, although a very simple turbulence model was used, as it is the original version of the Smagorinsky model, the calculated flow field presents an acceptable agreement with similar numerical results, and experimental data. Although the rms of the velocity fluctuations in the wake afar from the cylinder were under predicted, the Reynolds stresses have a reasonable prediction.

In contrast, the heat transfer prediction around the cylinder and the global values are not good. Even though the global Nusselt number have presented errors within $20 - 30\%$ in comparison with experimental values, that can not be considered as catastrofic, the distribution of the local Nusselt number has been poorly predicted around the cylinder. It is thought that this prediction can not be improved with flow prediction improvement only. But it seems that a better model for the turbulent thermal stress should be employed, and maybe also some new heat transfer modeling strategy. In other words, it seems that in order to improve heat transfer prediction, more information from the flow field it is necessary in the turbulent heat transfer modeling in this kind of turbulent flows.

5 APPENDIX

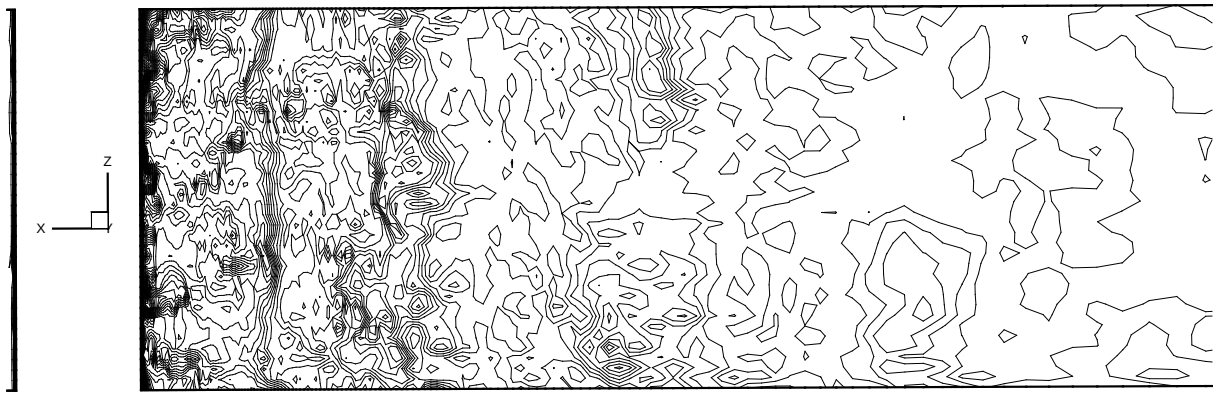

(a)

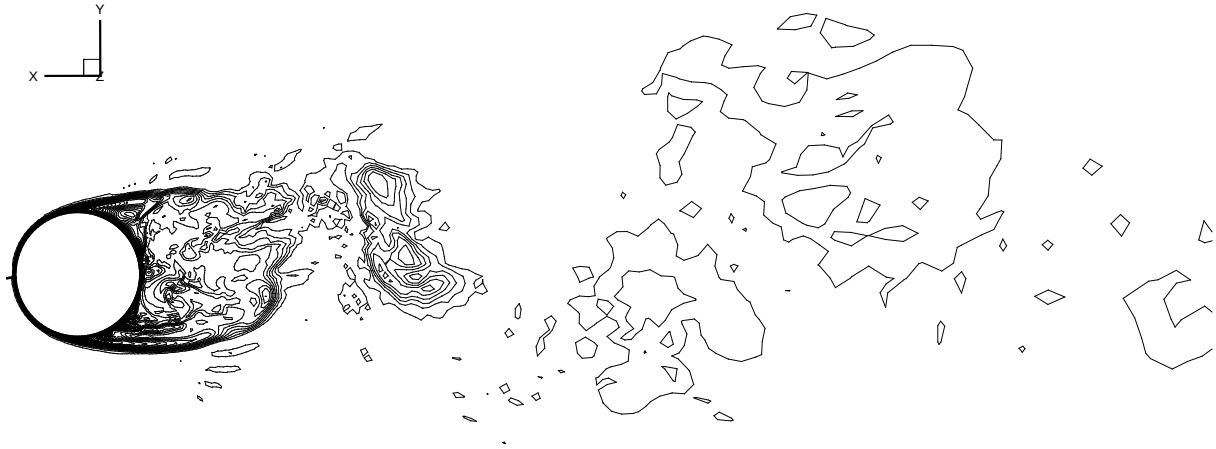

(b)

Figure 9: Instantaneous dimensionaless temperature field $\theta = (T - T_\infty)/(T_w - T_\infty)$ for RUN4. (a) In a $x - z$ plane at $y/D = 0$; (b) In a $x - y$ plane at $z/D = \pi$. 30 contours from 0 to 1.0.

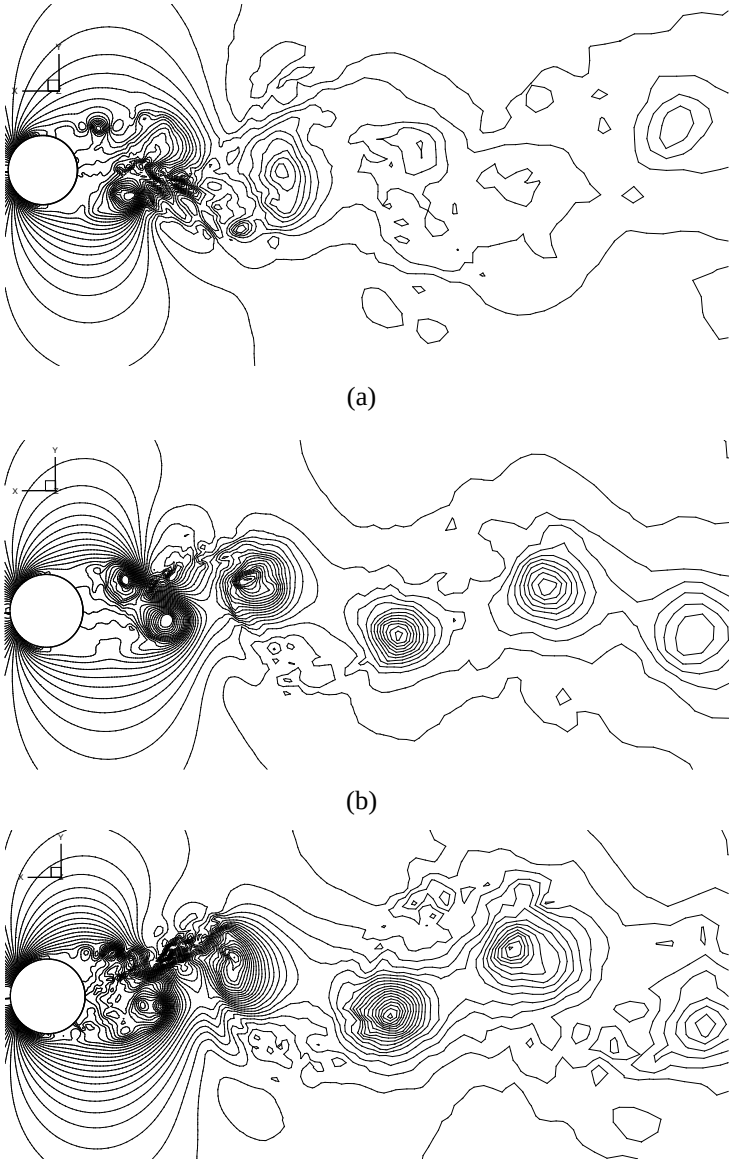

(a)

(b)

(c)

Figure 10: Instantaneous dimensionless pressure field $P/(\rho U_\infty^2)$ showing the importance of the numerical grid in the solution, at a $x-y$ plane at $z/D=\pi$. (a) RUN 2; (b) RUN 3; (c)RUN 4. 30 contours from -1.5 to 1.0.

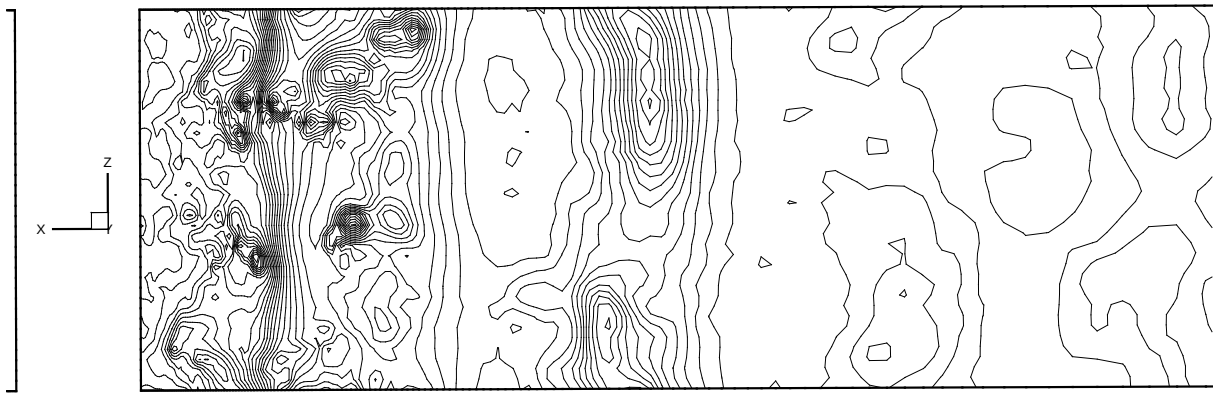

(a)

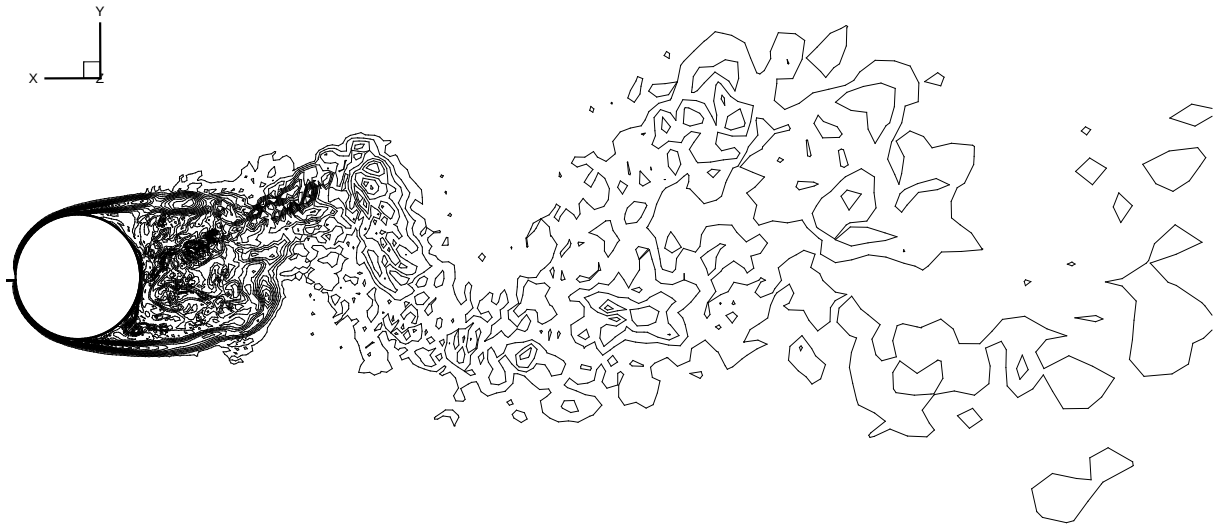

(b)

Figure 11: (a)Instantaneous dimensionless pressure $P/(\rho U_\infty^2)$ field showing the spanwise structures in the flow in a $x-z$ plane at $y/D=0$, revealing a need for a probably greater spanwise size of computational box. 30 contours from -1.5 to 1.0. (b)Instantaneous dimensionaless vorticity magnitude $\omega D/U_\infty$ field in a $x-z$ plane at $y/D=0$. 30 contours from 0 to 40.0.

ACKNOWLEDGMENT

This work was partially sponsored by the Air Force Office of Scientific Research under Grant No. FA9550-07-1-0393.

REFERENCES

Akselvoll. K, and P. Moin. Large-Eddy simulation of turbulent confined coannular jets and turbulent flow over a backward facing step. Report TF-63, Thermoscience Division, Department of Mechanical Engineering, Stanford University, 1995.

Beaudan, P. and P. Moin. Numerical Experiments on the Flow Past a Circular Cylinder at Sub-Critical Reynolds Number. *Report N. TF-62, Thermoscience Div. Det. of Mech. Engr.*, Stanford University, 1994.

Breuer, M. Large Eddy Simulation of the SUbcritical Flow Past a Circular Cylinder: Numerical and Modeling Aspects. *Int. J. Num. Meth. Fluids*, **28**, pp. 1281-1302, 1998.

Dennis S.C.R. and G.Z. Chang. Numerical solution for steady flow past a circular cylinder at Reynolds numbers up to 100. *J. Fluid Mech*, **42**, , pp. 471, 1970.

Catalano P., M. Wang, G. Iaccarino, and P. Moin. Numerical simulation of the flow around a circular cylinder at high Reynolds numbers. *Int. J. of Heat and Fluid Flow*, **24**, , pp. 463-469, 2003.

Fand R.M. Heat transfer by forced convection from a cylinder to water in crossflow. *Int. J. Heat Mass Transfer*, **8**, pp. 9951010, 1865.

Fornberg B. A numerical study of steady viscous flow past a circular cylinder. *J. Fluid Mech*, **98**, pp. 819, 1980.

Hansen R. P., and L.N. Long.Large-Eddy Simulation of a Circular Cylinder on Unstructured Grids, *AIAA 2002-0982*, 40th. AIAA Aerospace Sciences Meeting and Exhibit, Reno, 2002.

Inaoka J., J. Yamamoto, and K. Suzuki. Dissimilarity between heat transfer and momentum transfer in a disturbed turbulent boundary layer with insertion of a rod - modeling and numerical simulation. *Int. J. Heat Fluid Flow*, **20**, 290-301, 1999.

Kravchenko A.G., and P. Moin. Numerical studies of flow over a circular cylinder at $Re_D = 3900$. *Physics of Fluids*, **12**(2), 403-417, 2000.

Kong H, H. Choi, and J.S. Lee.Dissimilarity between the velocity and temperature fields in a perturbed turbulent thermal boundary layer. *Physics of Fluids*, **13**(5), 1466-1479, 2001.

Krall K.M., 1969, (data taken from Sarma and Surkhatme, 1977).

Knudsen J.D., and D.L. Katz. *Fluid Dynamics and Heat Transfer*, McGraw-Hill, New York, 1958.

Lourenco L.M., and C. Shih. Private communication, 1993 (data taken from Breuer, 1998).

Mittal R.. Large-Eddy simulation of flow past a circular cylinder. *Annual Research Briefs, Center for Turbulence Research*, 1995.

Nakmura H., and T. Igarashi. Variation of Nusselt number with flow regimes behind a circular cylinder for Reynolds numbers from 70 to 30 000. *Int. J. Heat and Mass Transfer*, **47**, 5169-5173, 2000.

Norberg C., (data taken from Kravchenko, and Moin, 2000).

Pasinato H.D. Some aspects of the numerical resolution of the unsteady incompressible Navier-Stokes equations, XI Congreso Argentino de Métodos Numéricos y sus Aplicaciones, Bariloche, 2000.

Perkins H.C., and G. Leppert. Forced convection heat transfer from a unifromlly heattd cylinder. *J. Heat Transfer*, **84**, 257-263, 1962.

Piomelli U. Large-eddy simulation of turbulent flows, TAM Report No. 767, UILU-ENG-94-6023, 1994.

Rajagopalan S., and R.A. Antonia, Flow around a circular cylinder–structure of the near wake shear layer, *Experiments in Fluids*, **38**, pp. 393-402, 2005.

Sanitjai S., and R.J. Goldstein. Forced convection heat transfer from a cicular cylinder in crossflow to air and liquids. *Int. J. H. Mass Transfer*, **47**, 4795-4805, 2004.

Sharma T.S., and Surkhatme. Local heat transfer from a horizontal cylinder to aie in cross flow: Influence of free convection and free stream turbulence. *Int. J. H. Mass Transfer*, **20**, 51-56, 1977.

Sholten J.W., and D.B. Murray. Unsteady heat transfer and velocity of a cicular cylinder in cross flow–I. Low freestream turbulence. *Int. J. H. Mass Transfer*, **41**(10), 1139-1148, 1998.

Son J., and T.J. Hanratty. Velocity gradient at the wall for flow around a cylinder at Reynolds number from 5×10^3 to 10^5. *J. Fluid Mech.*, **35**, 353-368, 1969.

Spalart P.R. and M.K. Strelets. Mechanisms of transition and heat transfer in a separation bubble, *Journal of Fluid Mechanics*. **403**, 329-349, 2000.

Schlichting H.. Boundary-Layer Theory, McGraw-Hill, 6th. Ed., New York, 1968

Tenneks H. and J.L. Lumnly. A First Course in Turbulence. *The MIT Press*, Cambridge, Massachusetts, 1972.

Young M.E., and A. Ooi. Comparative assesment of LES and URANS fro flow over a cylinder at Reynolds of 3900. *16th. Australian Fluid M. Conference*, Gold Coast, Australia, 2007.

Zukauskas A., and J. Ziugzda. Heat transfer of a cylinder in crossflow. Hemishere Pub., New York, 1985.